

Westinghouse Non-Proprietary Class 3

LTR-NRC-12-60 NP-Enclosure
TAC No. ME4700

**Response to the NRC's Request for Additional Information on WCAP-15942-P-A, Supplement 1,
"Material Changes for SVEA-96 Optima 2 Fuel Assemblies"(Non-Proprietary)**

August 2012

Westinghouse Electric Company
1000 Westinghouse Drive
Cranberry Township, PA 16066

© 2012 Westinghouse Electric Company LLC
All Rights Reserved

1. Based on the data provided for Zr-2 beta quench and []^{a,c} there does not appear to be a large advantage in performance of the former over the latter. What is the reason for the introduction of []^{a,c} and why would one be preferred over the other?

Answer:

The advantage of []^{a,c} channels is a []^{a,c} compared to Zry-2 channels, which is particularly important at high burn-ups. Even though beta quenched (β -Q) material eliminates the irradiation growth due to a randomized texture, the []^{a,c} in Zry-2 []^{a,c} in zirconium has been reached. The growth of β -Q material is thus []^{a,c} content. When the solubility limit of []^{a,c} at reactor temperature occurs (approximately []^{a,c}), the additional []^{a,c} will create a distortion due to the []^{a,c}. Whereas Zry-2 changes []^{a,c} at high burn-ups, []^{a,c} material is not expected to show []^{a,c} at high burnups, due to the []^{a,c}. Therefore, []^{a,c} channels are expected to experience less growth and channel bow than Zry-2 β -Q at high burn-ups.

[]^{a,c,™} is a trademark of Westinghouse Electric Company LLC, its Affiliates and/or its Subsidiaries in the United States of America and may be registered in other countries throughout the world. All rights reserved. Unauthorized use is strictly prohibited. Other names may be trademarks of their respective owners.

2. Sections 1.1 and 5.2.2 suggest that []^{a,c} only intended use for boiling water reactor (BWR) assembly components is for the outer channel and the []^{a,c}. Please confirm that these are the only applications of []^{a,c} for BWR assemblies.

Answer:

Westinghouse is only seeking approval from the NRC to use []^{a,c} material for the channels in BWR fuel, i.e. outer channel, cross sheet and reinforcement part (thicker bottom end part of channel), as stated in Section 5.2.2 of the supplement.

3. The amount of performance data for []^{a,c} is []^{a,c} Please provide additional data collected for []^{a,c} since the issuance of this topical and describe the plant application including operation in relation to the data, e.g., cladding temperatures, fluences, burnup, etc.

Answer:

Dimensional stability is one of the key factors in the development of channels for BWR fuel assemblies. ZrNbSnFe-alloys have very good dimensional stability during irradiation, i.e., the irradiation growth and creep rate are lower than for Zry-2 and Zry-4. The experience gained from irradiation of standard ZIRLO[®] material in PWRs shows that the growth of ZIRLO material is about []^{a,c} of the growth of Zry-4. This is the expected growth of ZIRLO channels in a BWR under the reasonable assumption that []^{a,c}

Based on Westinghouse's extensive experience with fabrication and in-reactor operating experience of ZrNbSnFe-alloys in PWRs to high burn-ups, demonstration []^{a,c} channels that have been inserted since 2004 are expected to achieve an assembly average burn-up of []^{a,c}

Channel Growth

The latest data for the channel growth in SVEA channels for all channel materials is shown in Figure 1. The graph contains data from both 12 and 24 month cycle operation with leading fuel assembly burn-ups of []^{a,c} channels up to approximately []^{a,c}

ZIRLO[®] is a registered trademark of Westinghouse Electric Company LLC, its Affiliates and/or its Subsidiaries in the United States of America and may be registered in other countries throughout the world. All rights reserved. Unauthorized use is strictly prohibited. Other names may be trademarks of their respective owners.



Figure 1. Channel Growth vs. Equivalent burn-up for Zry-4 α , β -Q Zry-4, Zry-2 α , β -Q Zry-2 and [redacted] channels.

Most length measurements have been made by an index plate and a zirconium alloy gauge whereas data indicated by "FCMS" (Fuel Channel Measuring System) was measured using a stainless steel gauge and temperature dependent correction factor.

For burn-ups above [redacted]^{a,c} the estimated irradiation growth of [redacted]^{a,c} channels is indicated in Figure 1. This estimation is based on [redacted]^{a,c} and [redacted]^{a,c} from [redacted]^{a,c} of [redacted]^{a,c} channel materials excluding [redacted]^{a,c}

The irradiation growth can be calculated since the hydrogen content and channel elongation are known. Table 1 contains the calculated irradiation growth for different channel materials used by Westinghouse. [redacted]

[redacted]^{a,c}

Table 1 Measured average hydrogen content of channel and outer channel elongation, predicted hydrogen induced elongation and irradiation growth due to the texture effect.

Material	Measured Hydrogen [ppm]	Predicted Growth due to H [mm]	Measured Channel elongation [mm]	Predicted Irradiation Growth [mm]
[Redacted Content]				

As a result, the irradiation growth for Zry-2 α channels is estimated to be []^{a,c} at []^{a,c} since the channel had a total elongation of []^{a,c} and the hydrogen content was approximately []^{a,c} which corresponds to []^{a,c} elongation due to []^{a,c}. For Zry-2 β -Q channel material the growth is []^{a,c}.

Finally, the irradiation growth for []^{a,c} channels is estimated to be []^{a,c} at []^{a,c}. This is reasonable since the hot cell examination of the average hydrogen content of the []^{a,c} channels is measured to []^{a,c} at []^{a,c}. The estimated average hydrogen pick-up after []^{a,c} is expected to be []^{a,c} than []^{a,c}, resulting in a channel elongation of []^{a,c}, which is approximately []^{a,c} less growth due to irradiation compared to Zry-2 α .

Furthermore, the high burn-up []^{a,c} NFIR BOR-60 program concluded that ZIRLO material growth was approximately []^{a,c} of Zry-2 α growth. This is in agreement with the above estimation of []^{a,c} reduction in overall growth of []^{a,c} channels compared to Zry-2 α at []^{a,c}.

Channel Bow

The channel bow is only a consequence of differential growth of the opposite sides of the channel. Since the channel growth is []^{a,c} for []^{a,c} channels than for Zry-2 α and Zry-4 α channels the corresponding channel bow is []^{a,c} for []^{a,c} channels as the in-pile measurement as shown in Figure 2.



Figure 2. Channel Bow in Symmetric Lattice vs. Equivalent burn-up for Zry-4 α , β -Q Zry-4, Zry-2 α , β -Q Zry-2 and []^{a,c} channels

Channel Oxide

The maximum channel oxide thickness for SVEA channel is traditionally evaluated by []^{a,c} and is shown in Figure 3 a. The operating condition with early control rod history i.e. 24 month operation gives the highest oxide growth for []^{a,c} and []^{a,c} for []^{a,c} channels. Under such conditions the maximum average oxide thickness is between []^{a,c} for []^{a,c} channels and for Zry-4 β -Q approximately []^{a,c} at a burn-up of about []^{a,c}. The maximum oxide thickness in Figure 3 a is expected to be []^{a,c} at []^{a,c} burn-up of []^{a,c} since no additional control rod exposure is experienced during its last cycles. In Figure 3 b the average oxide thickness is shown, which is []^{a,c}

a,c



Figure 3a and 3b. Channel Oxide thickness vs. Equivalent burn-up for β -Q Zry-4, Zry-2 α , β -Q Zry-2 and []^{a,c} channels. Figure 3a shows the maximum oxide and Figure 3b shows the average oxide []^{a,c}

For operating conditions without control rod history on channel sides []^{a,c} the []^{a,c} channel has a []^{a,c} oxide growth of approximately []^{a,c}, while the control rod side []^{a,c} has a []^{a,c} with a []^{a,c} oxide thickness of approximately []^{a,c} as Figures 4 a and b show. The data in Figure 4a is the []^{a,c} and data in Figure 4b is the []^{a,c} The oxide growth on the control rod side is typically shadow corrosion, which is not expected to have any significant growth later in life as indicated by the prediction curve, i.e. []^{a,c}

a,c



Figure 4a and 4b. Channel Oxide thickness vs. Equivalent burn-up for β -Q Zry-4, Zry-2 α , β -Q Zry-2 and []^{a,c} channels. Figure 4a shows side 2 and 3 and Figure 4b shows side 1 and 4.

The highest oxide thickness for a Zry-2 β -Q channel is a []^{a,c} side with data from the []^{a,c} of the channel. The data points from the Zry-2 β -Q channel with a red

border around the data points are all from one reactor with the highest measured average oxide thickness, which can also be observed in the previous figure, Figure 3a and 3b.

Channel Bulge

Channel bulge occurs due to the differential pressure between the inside and the outside of the channel and is dependent on the creep properties of the zirconium alloy (see also answer to RAI-6). The bulge for SVEA channels []^{a,c}
Therefore it is not a critical property for the SVEA channel design.

The creep performance for cladding material in RXA condition has been measured and concluded to be []^{a,c} for ZIRLO materials than for Zry-4 α (PWR) and Zry-2 α (BWR) material. Zry-2 α -material is therefore expected []^{a,c} channel creep.

4. The data from lead test assemblies (LTAs) have been taken from []^{a,c} plants. Have these plants and subsequent plants with LTAs been limiting in terms of channel corrosion, growth and/or bow than other plants? Please discuss the performance of channels in these plants to those in limiting plants.

Answer:

Data originally came from []^{a,c} plants, however the LTA data today comes from []^{a,c} plants, see Table 2. The data from leading fuel assemblies ([]^{a,c}) is from []^{a,c} representative plants: []^{a,c}.

[]^{a,c} operates on 24 month cycles with early control, which is considered the limiting operating condition for channel corrosion occurring early in life with a small gap between channel and control rod (S-lattice). []^{a,c} is representative of ordinary 12 month cycle operation.

SVEA []^{a,c} channels have been delivered since 2004 to []^{a,c} different reactor types/environments and operating conditions. The different deliveries are shown in Table 2.

Table 2 | *[]^{a,c} Channel deliveries*

a,c

Fuel inspections have been conducted in []^{a,c} reactors. The first in-pile measurements were made in []^{a,c} in 2005 after []^{a,c} cycle and in 2009 after []^{a,c} cycles. Inspections after []^{a,c} annual cycles in []^{a,c} were performed during 2010 and 2011. Inspections after []^{a,c} and []^{a,c} months of operation in []^{a,c} were performed during 2009 and 2011 with anticipated results of []^{a,c}. Additional inspections of []^{a,c} channels will be performed during the upcoming years in

order to verify the [and environments.

] ^{a,c} channel performance in different operating conditions

5. The following are related to growth of []^{a,c}.

- a. Do the analytical models for channel growth account for individual effects due to hydriding, irradiation, and creep or is there one growth model that incorporates all of these effects implicitly? If the latter is true then a change in channel corrosion/hydriding or stress will change channel growth without changes in channel material. Therefore, a change to water chemistry or assembly design could change channel growth from previous experience. How does Westinghouse intend to control these potential effects on growth that are independent of the channel material? If the growth is dependent on individual model effects please provide an example analysis of how these individual model effects are included in a total growth.

Answer:

There is only one upper bound channel growth prediction for SVEA channels. This growth prediction is empirical and is based on the complete SVEA channel growth database, which covers a wide range of operating conditions (such as different water chemistries) from many different applications. The channel growth prediction of []^{a,c} is conservatively chosen for modern channel materials (see Figure 1 in the answer to RAI-3).

There are no significant axial forces acting on the SVEA channel during operation. A difference between the “shopping bag design” of the SVEA fuel compared to other fuel designs with the channel hanging from the top tie plate, however, is that for SVEA fuel, gravity acts as a compressive force on the channel and thus reduces channel growth.

Channel growth is routinely measured at irradiated fuel inspections. Results are added to and evaluated against the channel growth database. Current data for []^{a,c} channels falls well within the current database.

- b. The axial growth of []^{a,c} than for Zr-2 RXA material. This could affect the clearance between the sub-bundle and the frame (channel) of the handle assembly. Please discuss the impact of []^{a,c} channel growth on this clearance.

Answer:

[]^{a,c} is conservatively assumed, combined with []^{a,c} growth along with []^{a,c} when evaluating margin for unrestricted sub-bundle growth in the fuel channel. The analysis in Section 4.2.2 of Reference 1.6, where sufficient margin is shown also with zero channel growth, is thus unaffected by introduction of []^{a,c} channels.

6. Please confirm that the channel creep data in Figure 4.2-5 is only from Zr-2 channels and no []^{a,c} channel creep data are presented. Section 4.2.1 page 4-4 suggests that []^{a,c} and Zr-2 (RXA) will have []^{a,c} irradiated creep rate. Please provide justification to substantiate this claim. Please provide data on the irradiated creep rate of []^{a,c} compared to that for Zr-2 (RXA) along with a discussion of the impact of differences in channel creep rate on in-reactor performance.

Answer:

The channel creep deformation data in Figure 4.2-5, intended to show the conservative nature of this general channel creep prediction model, is from []^{a,c} Zry-4 channels. The response to RAI-14 in Reference 1.6 further discusses the creep model and the application for Zry-2 material and SVEA-96 Optima2 fuel in US BWRs. No []^{a,c} channel creep data is provided in Figure 4.2-5.

The thermal creep as well as the irradiation creep is dependent upon chemical composition and final metallurgical condition (SRA, pRXA, RXA). []^{a,c} however a study on []^{a,c} has been performed and the results show that the thermal creep for []^{a,c} give a []^{a,c} creep rate for []^{a,c} cladding compared to standard Zry-2, as shown in Figure 5. This comparison is relevant since []^{a,c} which is the same condition as the sheet material.



Figure 5 Creep behavior for Std LK3 liner (RXA) and []^{a,c} Cladding tubes

The in pile creep performance for []^{a,c} material compared to Zry-2 α will be measured on irradiated channels []^{a,c} in order to confirm the []^{a,c} channel creep performance. Bulge measurements were recently made for Zry-2 β -Q and

[]^{a,c} channels in []
measured to maximum []

[]^{a,c} MWd/kgU and the creep was []
[]^{a,c}.

7. An example of geometric compatibility with other fuel types at []^{a,c} is provided on pages 4-5 and 4-6. This example assumes []

[]^{a,c} However, it appears that the limiting condition for compatibility will be []

[]^{a,c} Is this interpretation correct? If so please discuss the impact of []^{a,c} on compatibility between the []^{a,c} of the two different assemblies.

Answer:

This interpretation is not correct. The different fuel assembly designs have different lengths at BOL, so []^{a,c} for the SVEA assembly might not be the limiting condition. []^{a,c} must be considered.

The conservative Westinghouse methodology for evaluation of geometric compatibility with other fuel types []

[]^{a,c} These combinations are included in the sample application in Section 4.2.1 of Reference 1.6. Since the introduction of []^{a,c} channel material does not change the assumptions concerning SVEA channel growth, i.e. []^{a,c}, the sample application in Reference 1.6 is unaffected by the introduction of []^{a,c} channels and is thus not included in the supplement.

8. The following are related to channel bow.

- a. How is []^{a,c} determined? Provide an example with data for both asymmetric and symmetric lattices. Why is the []^{a,c} for evaluating control blade insertion?

Answer:

During NRC review of Reference 1.6 and prior to introduction of SVEA-96 Optima2 in US BWR plants, a modified methodology for evaluation of channel bow and its effect on channel compatibility with the control rod was introduced (see the response to RAI-15 in Reference 1.6.) The modified methodology included an extensive statistical evaluation of the Westinghouse SVEA-10x10 channel bow database, including previously used Zry-4 channel material. Control rod []

[]^{a,c} was used as a reference to bound a similar evaluation for each US application concerning the risk of control rod maneuvering issues with SVEA-96 Optima2 fuel. Data was also provided to the NRC during the review of Reference 1.6 for independent evaluations.

Figure 6 shows the current Zry-2 channel bow database for a symmetrical core lattice, including a new statistical evaluation. []^{a,c} have been calculated for intervals of []^{a,c} (first interval []^{a,c}, second interval []^{a,c} etc) and each interval is represented by []^{a,c} the interval. The average bow is, []^{a,c}

In the current methodology presented in RAI-15 of Reference 1.6, the statistically calculated channel bow toward control rod of []

[]^{a,c} is used for symmetric lattice and is also indicated in Figure 6. This figure also shows the conservatism in using []^{a,c} data for Zry-4 in []^{a,c} at []^{a,c} as input in the analysis for SVEA-96 Optima2 with the current Zry-2 channel material.

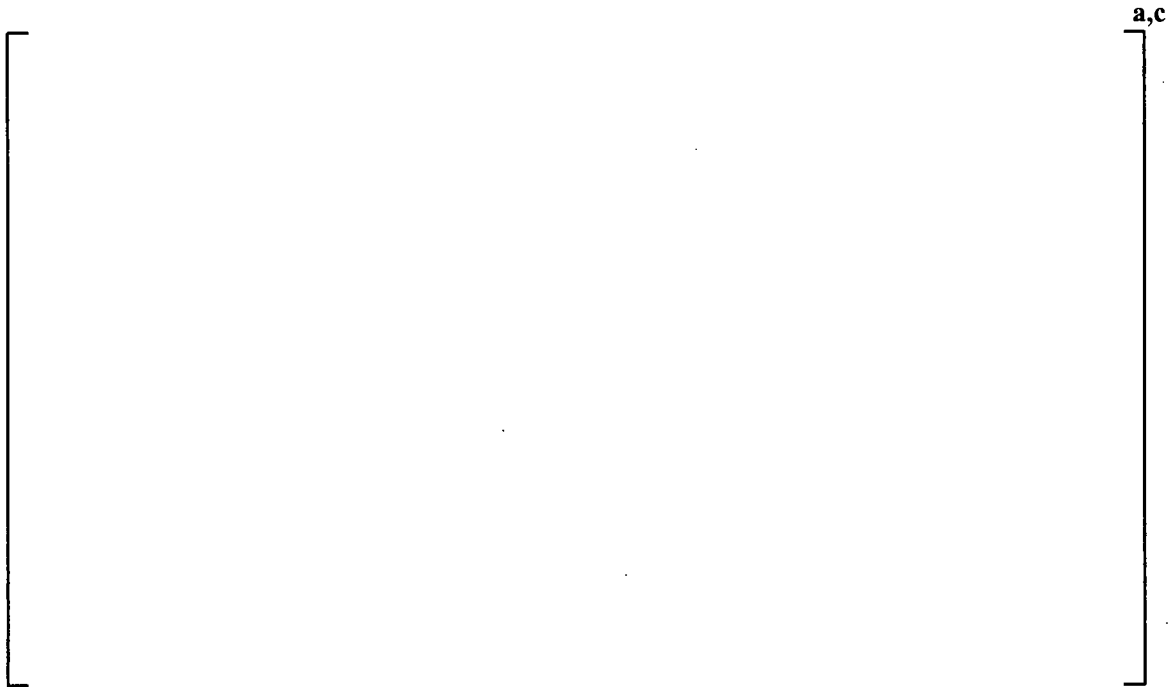


Figure 6. Channel bow vs. burnup for symmetric lattice.

The number of data points for []^{a,c} channel bow is, []^{a,c} as can be seen in Figure 2-15 and 4.2-6 of the supplement, the []^{a,c} channel data falls within current channel bow database, for which successful and extensive operating experience exist. Therefore, introduction of []^{a,c} channel material is not expected to []^{a,c} concerning channel bow and risk of control rod maneuvering issues. []^{a,c} channels are expected to show []^{a,c} than current Zry-2 and previous Zry-4 channels and therefore, current operating experience and methodology conservatively bounds []^{a,c} channels in US applications.

The database for channel bow in an asymmetric lattice is still limited although the operation experience is extensive; with more than 3000 SVEA-96 Optima2 assemblies delivered to []^{a,c} and []^{a,c}. More datapoints from []^{a,c} would be needed []^{a,c} for channel bow increase with burn-up in an asymmetric lattice. However, the database for channel bow in a symmetric lattice, shown in Figure 6 above and also in Figure 2-15 of the supplement, has good coverage approaching []^{a,c} and the channel bow drivers are the same irrespective of lattice symmetry. The difference in water gap width in an asymmetric lattice however causes a bias in average channel bow when compared to a symmetric lattice. The average channel bow in the asymmetric lattice in Figure 4.2-6 is about []^{a,c}, while the average

channel bow in the symmetric lattice in Figure 2-15 is []^{a,c}. Except for this bias, there is no reason to suspect that the channel bow behavior toward the control rod in an asymmetric lattice should be significantly different than for a symmetric lattice. The channel bow behavior in a symmetric lattice was thoroughly evaluated in the response to RAI-15 of Reference 1.6 and the database for Zry-2 and also []^{a,c} channels in a symmetric lattice is still within previous experience with Zry-4 channels concerning bow toward the control rod and for which extensive and completely successful experience exist.

b. An example analysis example is provided on page 4-10 that assumes []

] ^{a,c} However, examination of the data in Figure 4.2-6 []^{a,c} suggests that the increase in bow []^{a,c} Please provide a discussion on why []^{a,c} should not be assumed and the potential impact []^{a,c} would have on control blade interference.

Answer:

The applicability of current methodology to asymmetric lattice as well as the operating experience of SVEA-96 Optima2 fuel in asymmetric lattice is discussed in the response to RAI-8a above.

The methodology for compatibility with the control rod according to RAI-15 of Reference 1.6 includes []

] ^{a,c} and assumes [] ^{a,c} of channel bow [] ^{a,c} with burn-up, based on previous experience with Zry-4 channels in [] ^{a,c} BWR/6 when calculating a [] ^{a,c} channel bow towards control rod at EOL.

However, the input used in the methodology is []

] ^{a,c} and, as can be seen in Figure 6, []

] ^{a,c} of the database for current Zry-2 channels. Furthermore, the basis for the current methodology is an entirely successful operating experience concerning control rod maneuvering, with [] ^{a,c} as the reference plant in the analysis. This basis has been strongly reinforced since the methodology in RAI-15 of Reference 1.6 was introduced and approved.

Today there is even stronger evidence by extended operating experience and control rod slow to settle tests that supports the conservatism of the current methodology concerning control rod maneuverability.

9. The following are related to hydrides in []^{a,c}.
- a. Section 4.2.9 assumes []^{a,c} for hydrogen pickup for evaluating channel performance, however, recent high burnup data from Zr-2 BWR fuel rods suggest that the hydrogen pickup increases exponentially above a local burnup of 45 GWd/MTU (see paper by K. Geelhood and C. Beyer entitled "Hydrogen Pickup Models for Zircaloy-2, Zircaloy-4, M5 and ZIRLO™," 2011 Water Reactor Fuel Performance Meeting, Chengdu, China September 11-14, 2011; also see paper by E. V. Mader et al entitled "EPRI BWR Channel Distortion Program" at the same meeting). Please provide a discussion on significant difference of these two hydrogen pickup models for []^{a,c} and Zr-2 (RXA).

Answer:

Zry-2 and Zry-4 change its hydrogen pick up significantly at high burn-up due to the dissolution of Secondary Phase Particles. The []^{a,c} material contains []^{a,c}, and therefore []^{a,c} hydrogen pick up at high burn-up is expected. Available data is consistent with this view.

- b. Page 4-18 provides a limit on hydrides in []^{a,c}. There is some evidence that Zr-2 RXA is embrittled at hydrogen levels below those proposed as limits for []^{a,c}. Please provide ductility data (based on uniform elongation and yield strength) from irradiated []^{a,c} up to the hydrogen limit requested.

Answer:

When a comparison is made between []^{a,c} material and Zry-4, it shows that the []^{a,c} for []^{a,c} channels due to the irradiation hardening is similar to that for Zry-4.

The axial tensile tests were performed at []^{a,c} in air. Tensile specimens were prepared from the channel samples by []^{a,c} with tension direction oriented []^{a,c} to the []^{a,c} direction of the channel, see Table 3.

Table 3 Un-irradiated and irradiated mechanical properties for []
material

] ^{a,c} a,c

[]

The increase of test temperature from [] ^{a,c} resulted in a [] ^{a,c} of ultimate tensile strength (Rm) from [] ^{a,c} to approximately [] ^{a,c}. The effect of test temperature on material ductility was [] ^{a,c} pronounced going from [] ^{a,c} to [] ^{a,c}.

The increase in tensile properties for Zirconium alloys during irradiation are described in different ASTM reports, e.g. in Ref [1] "Effect of Irradiation at 588K (315°C) on mechanical properties and Deformation behaviour of Zirconium Alloy Strip" it is reported that yield strength of Zry-4 material in RXA condition increases from 385 MPa to 720 MPa after an irradiation fluence of 5×10^{20} n/cm² (E>1MeV). The data at room temperature is summarized in Table 4 which shows the tensile test result in both the longitudinal and transversal direction.

Table 4. Un-irradiated and irradiated mechanical properties at RT for Zry-4 strip, Ref [1]

Material	Fluence [n/cm ²] (E>1MeV)	Longitudinal Direction			Transverse Direction		
		Yield Strength [MPa]	Tensile Strength [MPa]	Total Elongation [%]	Yield Strength [MPa]	Tensile Strength [MPa]	Total Elongation [%]
RXA	0	385	470	30	395	440	32
RXA	5×10^{20}	720	720	3	735	735	2,8

At elevated temperature (315°C) the yield strength of Zry-4 RXA increased from 146 MPa to 474 MPa after an irradiation fluence of 5×10^{20} n/cm² (E>1MeV). Data for both the longitudinal and transverse direction at elevated temperature is presented in Table 5.

Table 5 Un-irradiated and irradiated mechanical properties at 315°C for Zry-4 strip, Ref [1].

Material	Fluence [n/cm ²] (E>1MeV)	Longitudinal Direction			Transverse Direction		
		Yield Strength [MPa]	Tensile Strength [MPa]	Total Elongation [%]	Yield Strength [MPa]	Tensile Strength [MPa]	Total Elongation [%]
RXA	0	146	206	35	154	190	36
RXA	5x10 ²⁰	474	476	5	472	472	4,6

It can be concluded that the []^{a,c} in []^{a,c} and []^{a,c} in []^{a,c} for []^{a,c} channels due to the irradiation hardening is []^{a,c} as for Zry-4

10. The submittal requests that []^{a,c} be substituted for []^{a,c}. The topical report states (Section 2.2) that the former and latter []^{a,c} have similar corrosion resistance including that due to shadow corrosion. Please provide a comparison of []^{a,c} shadow corrosion data along with a discussion for []^{a,c}. Is the secondary phase particle (SPP) size controlled for []^{a,c}? If not why not when it is known that SPP is important for controlling nodular corrosion.

Answer:

Shadow corrosion comparison between []^{a,c} and []^{a,c} material have been made for channel material []^{a,c}.

[]^{a,c} The shadow corrosion is shown to be []^{a,c} for both []^{a,c} and []^{a,c} material, both for []^{a,c} and []^{a,c}, as shown in Figure 7.

The processes of both Zry-2 β-Q and Zry-2 α material are qualified processes and are reproducible for each product with defined []^{a,c} that control the SPP sizes for each product.



Figure 7. Comparison of oxide thickness of []^{a,c}

11. Please provide a description the new strength specifications for []^{a,c} along with the []^{a,c} for channel application. Also, provide an analysis for limiting normal operation and anticipated operation occurrence events involving case of channel overpressure.

Answer:

WCAP-15942-P-A, Supplement 1 has been updated to include the data and analysis requested. The revised WCAP is attached to this transmittal and has been renumbered as "WCAP-15942-P-A, Supplement 1, Revision 1". Upon approval, it will be numbered as "WCAP-15942-P-A, Supplement 1, Revision 1-A," consistent with the numbering system employed originally. An abstract will be added to the approved version explaining why this revision was necessary.

REFERENCE

- [1] P. Morize et. al., "Effect of Irradiation at 588K (315°C) on mechanical properties and Deformation behavior of Zirconium Alloy Strip," ASTM STP 939.